Using TMS-EEG to study the intricate interplay between GABAergic inhibition and glutamatergic excitation during reactive and proactive motor inhibition

Tingting Zhu[a], Chenglong Cao[b], James Coxon[c], Alexander T. Sack[a], Inge Leunissen[a]*

[a] Department of Cognitive Neuroscience, Faculty of Psychology and Neuroscience, Maastricht University, Maastricht 6229 EV, Netherlands

[b] Department of Neurosurgery, The First Affiliated Hospital of University of Science and Technology of China, Hefei, China

[c] School of Psychological Sciences, Monash University, Clayton 3800, VIC, Australia

*Corresponding author

Email address: inge.leunissen@maastrichtuniversity.nl

Abstract

Background: Combining Transcranial magnetic stimulation (TMS) with electroencephalography (EEG) enables assess TMS-evoked potentials (TEP) and estimate γ-aminobutyric acid (GABA) and glutamatergic neurotransmission across the entire motor inhibition network. The N45 and N100 TEP peaks are associated with GABAa and GABAb signaling, respectively, whereas the N15, P30 and P60 TEPs reflect glutamatergic neurotransmission. This study applied TMS-EEG to investigate modulation of TEP components during reactive and proactive inhibition and whether individual differences in GABA and glutamate signaling predict inhibitory performance.

Methods: Twenty-four healthy participants completed two TMS-EEG sessions, targeting either the left primary motor cortex (M1) or the pre-supplementary motor area (preSMA) at rest and during a stop-signal task. We compared TEP peak amplitudes across TMS (active/sham) and Trial Type (stop/go trials) and assessed their relationship with task performance.

Results: Participants with a higher N45 amplitude at rest over M1, reflecting increased GABAa signaling, demonstrated a faster stop-signal reaction time. TMS during motor inhibition revealed higher N15 amplitudes over preSMA, reflecting increased glutamatergic neurotransmission, for successful stops versus go trials. Similarly, N15 was higher for uncertain than certain go trials suggesting that an early excitatory signal from preSMA is crucial for both reactive and proactive motor inhibition.

Conclusion: Higher GABAa inhibitory signaling in M1 at rest is linked to faster reactive inhibition. The preSMA likely plays a key role in both reactive and proactive motor inhibition. Here we provide novel direct empirical insights into the underlying neurophysiological mechanisms, highlighting a functional relevance of early glutamatergic excitatory signals for successful motor inhibition.

Keywords: TMS-evoked potential, GABA, motor inhibition, stop-signal task

Introduction

Motor inhibition, an essential function in daily life, refers to the ability to suppress initiated movements, particularly when execution is undesirable [1, 2]. Two variants of motor inhibition can be distinguished, reactive and proactive inhibition [3]. While reactive inhibition represents motor suppression in reaction to an unexpected stop signal during an ongoing movement, proactive inhibition refers to a preparatory process that facilitates movement cancellation when one might be required to stop soon. The putative neural underpinnings involve complex interactions within a fronto-basal ganglia network, wherein the right inferior frontal cortex and pre-supplementary motor area (preSMA) instigate inhibition of thalamo-cortical output via the indirect and hyperdirect cortico-basal ganglia pathways [4].

Given the prominent role of the primary motor cortex (M1) in shaping descending motor output, M1 is likely the site where movement preparation and cancellation meet [5]. Single-pulse transcranial magnetic stimulation (spTMS) studies revealed that cortical excitability as measured by motor evoked potentials (MEP) is reduced in M1 during movement cancellation [6-9], but this reduction of MEPs could be the consequence of either an active inhibition process or a reduction of excitation. Subsequent paired-pulse TMS (ppTMS) studies demonstrated that motor inhibition indeed coincided with an increase in short intracortical inhibition (SICI) [7, 10], and that the degree of this increase relates to the speed of the inhibition process [11]. This supports that movement cancellation requires an active inhibition process at the level of M1 brought about by an increase in GABAa signaling.

The GABAa receptor is a fast-acting ligand-gated chloride channel that quickly inhibits signals via postsynaptic membrane hyperpolarization, while the GABAb receptor produces prolonged inhibitory effects by G-protein-coupled modulation of intracellular signaling pathways [12]. It is tempting to map this distinction between the receptor types to the fast reactive inhibition versus prolonged proactive inhibition. GABAb-mediated intracortical inhibition in M1 can also be assessed with ppTMS as long intracortical inhibition (LICI). LICI is indeed increased when a stop signal might appear [13]. However, there are also some indications that GABAb signaling is relevant for reactive inhibition, with the cortical silent period prolonged during successful inhibition [8]. When measured at rest, the silent period, LICI, and SICI all relate to inhibitory task performance [14-16]. Measuring LICI during the inhibition process is difficult due to the long interval between the conditioning and test pulses. A potential solution to achieve a more comprehensive understanding of GABAergic neurotransmission during motor inhibition, is to combine TMS with electroencephalography (EEG).

The TMS-evoked potential (TEP) in the EEG signal [17-21] contains a series of peaks, reflecting the excitability and reactivity of the underlying cortical networks [22, 23]. Whereas the N15, P30 and P60 peaks are believed to reflect excitation [20, 24, 25], the N45 and N100 have been linked to GABAa dependent and GABAb receptor-mediated neurotransmission, respectively [20, 26, 27]. An earlier spTMS-EEG study found increased N100 amplitude during successful reactive inhibition [28],

suggesting GABAb involvement in motor inhibition. Yet, methodological limitations such as a small sample size (N = 6) and lack of a sham condition limit the generalizability of these results.

A major advantage of TMS-EEG is that the assessment of intracortical inhibition and facilitation is no longer limited to M1. Therefore, our study aims to investigate changes in inhibition and excitation during reactive and proactive inhibition by applying a spTMS-EEG protocol targeting either preSMA or left M1 in separate sessions. For M1, we hypothesized that the amplitude of the N45 peak (reflecting GABAa) will be amplified specifically during successful stopping (i.e., reactive inhibition), whereas the N100 peak may exhibit differences already at the start of the trial, indicating the involvement of the slower GABAb system in proactive inhibitory control. The preSMA sends an excitatory signal to the subthalamic nucleus (STN) and striatum when there is a need for inhibition which might result in higher N15, P30 or P60 amplitudes (reflecting glutamate) during reactive and/or proactive inhibition. Understanding the intricate interplay between GABAergic inhibition and glutamatergic excitation can contribute to a better understanding of the mechanisms of motor inhibition and provide valuable insights into potential treatments for neurological and psychiatric disorders with inhibitory dysfunction.

Material and methods

Subjects

Twenty-five healthy participants were recruited for this study (11 males, age range: 19-31, mean age: 25.56 ± 4.35). The inclusion criteria were: (i) right-handed (mean laterality quotient: 97.5 ± 5.95, as assessed by the Oldfield handedness inventory [29]); (ii) no history of neurological disorders (such as epilepsy, seizure or stroke) or neuropsychiatric disorders; (iii) no history of alcohol or other drug abuse/dependence; and (iv) no TMS and MRI contraindications, such as the metal implants [30]. All participants gave their written informed consent and were remunerated for their participation. The experimental procedure was approved by the local ethics committee.

Experimental design

The study consisted of three separate sessions, conducted on different days. In the first session, we obtained a structural MRI, and a 12-min stop-signal task (SST) assessment was carried out to measure participants' baseline inhibitory performance. During the second and third sessions (minimally 48h apart, range = 48 - 435 h, mean = 213 ± 123 h), participants underwent TMS-EEG targeting either preSMA or M1. TMS was applied at rest (2 blocks: 1 active stimulation and 1 sham) and during SST

performance (4 blocks: 2 active stimulations, 2 sham). The order of the active and sham stimulation was counterbalanced over participants but kept the same for both targets within subjects.

MRI data acquisition

A structural MRI was acquired for every participant to navigate the TMS coil. MR scanning was performed on a Siemens Prisma 3T scanner with the following parameters: 192 sagittal slices, TR = 2300ms, TE = 2.98ms, FOV = 256 × 256 mm^2, voxel size = 1 mm×1mm×1mm, flip angle = 9°.

Stop-signal Task paradigm

An anticipatory response version of the SST, programmed in LabView (2020), was used to assess motor inhibition (Figure 1). Participants were seated ~1m from a 240Hz screen. The display consisted of a vertical bar that ascended at a constant speed, reaching the top in 1000ms. Participants were instructed to press a button (right index finger) to halt the bar at the target line (800ms) as accurately as possible during go trials. In 25% of trials, the bar unexpectedly stopped before the target line. In these stop trials participants were expected to withhold their response. A staircasing algorithm kept P(inhibit) ≈ 50% (initial stop time 200ms from target, 25ms steps). We instructed participants to give response for go trials as accurate and fast as possible, and it would not be possible to withhold the button press on all stop trials. Participants performed two practice blocks: 20 go trials, then 20 trials comprising stop and go trials. The task commenced with 40 go only trials (light blue bar, certain go trials), followed by 200 trials (dark blue bar) comprising 150 go trials (uncertain go trials) and 50 stop trials randomly intermixed. The inter-trial interval (ITI) ranged from 3 to 4 seconds.

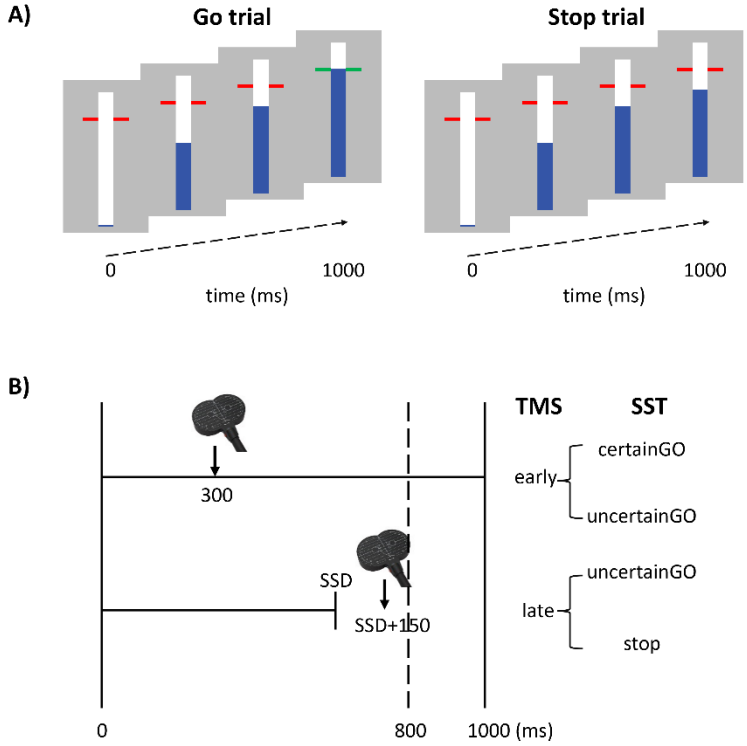

Figure 1. Stop-signal task paradigm with timing of TMS and conditions of interest. (**A)** The anticipatory version of the SST display with mixed go and stop trials. Participants were asked to halt an ascending bar at the target line during go trials. Feedback was given based on response timing (green <20ms, yellow <40ms, orange <60ms, or red >60ms from target). Stop trials required response withholding when the bar stopped earlier than the target line, but the feedback of the stop trials remained red. (**B**) Experimental design indicating the timing of TMS pulse on SST trials. The arrow presents the time when TMS pulse was given. The early TMS was administered 300ms after trial onset, while late TMS pulses occurred 150ms after the stop signal delay (SSD). For go trials the average SSD for each participant was used, whereas for stop trials TMS occurred 150ms after the SSD of the current trial. The early TMS condition occurred on both certain and uncertain go trials, but the late TMS occurred on uncertain go and stop trials.

TMS-EEG set-up

EEG was recorded with 64 low-profile electrodes (Braincap-TMS, Easycap GmbH) linked to a BrainAmp DC Amplifier (Brain Products, GmbH) with ground electrode located at FPz and the online reference at TP10. Electrooculography signals were recorded with 2 bipolar channels capturing horizontal and vertical eye movements. Data was recorded from DC with a sampling rate of 5 kHz and impedances below 5 kΩ. The electrode leads were oriented perpendicular to the coil handle. Polymeric

foam spacers (~0.5 cm high) were placed on the EEG cap to avoid direct contact of the TMS coil with EEG electrodes and to minimize bone conduction of the TMS click [31].

Biphasic TMS pulses were delivered using a MagPro-X100 Stimulator with a 70 mm figure-of-eight coil in a P→A current direction (MC-B70, MagVenture A/S, Farum, Denmark). The FDI motor hotspot located at which five consecutive TMS pulses produced the highest mean motor evoked potential (MEP), coil 45° to the midsagittal plane, handle pointing posteriorly. The motor hotspot was marked on the cap and captured with a neuronavigation system (Localite TMS Navigator 3.0.63, SW-Version3) to ensure optimal positioning during the M1 session. Next, resting motor threshold (RMT) was determined as the lowest stimulus intensity that elicited five out of ten MEP ≥ 50 µV (peak to peak) [32]. PreSMA was defined as MNI coordinate (11, 10, 62) [33, 34] and transformed to subject space for neuronavigated targeting with the handle was oriented posteriorly [35]. The stimulation intensity was set at 100% RMT and decreased by 1-2% on M1 if interference with index finger extension was observed or self-reported by the participant. During sham stimulation, a 4cm polyethylene foam was attached to the bottom of the coil to prevent any transfer of active TMS pulses to the scalp [36].

We took measures to reduce somatosensory and auditory TEP contamination. The sound of the TMS coil was masked by administering adaptive white noise with the same frequency of the TMS click through in-ear headphones fitted inside foam earplugs (E-A-RTONE 3A Earphones) [36-38]. Additionally, we applied Cutaneous Electric Stimulation (CES, DS7A Digitimer Ltd, USA) [39] [36, 38, 40, 41] (see supplementary info for more details). White noise and CES were applied during both active and sham TMS.

Participants were asked to fill out the visual analog scale (VAS, scale 1 to 10) after each block, referring to the perceived sound and sensation. The VAS included the following items: 1) intensity of white noise; 2) intensity of scalp sensation; 3) area of scalp sensation; 4) pain or discomfort intensity [38]. Extra items were applied only after the whole experiment: 1) comfort of the sound; 2) differences between blocks.

TMS at rest

Participants were asked to sit comfortably, be at rest and avoid any systematic thinking. They were instructed to fixate on a white cross on the screen during TMS at rest (rsTMS) block. Seventy-five consecutive TMS pulses with different ITI (4/4.5/5s) were transferred for each rsTMS block (1 active and 1 sham stimulation), lasting for about 6 mins. The target site was kept the same for rest and task within each session.

TMS during stop-signal task performance

Per session, the SST with TMS included 160 certain go trials, 480 uncertain go trials and 160 stop trials (total = 800 trials) divided over 4 task blocks (2 active and 2 sham stimulation blocks). The TMS pulse was randomly applied at two different time points: early (i.e., 300ms after trial onset) or late (i.e., participant-specific stop time + 150ms) (Figure 1). The late stimulation point was chosen because active inhibition is expected 150ms after presentation of the stop-signal [7]. The participant-specific stop time was determined from the no-TMS session with the formula: 800ms – [mean (GoRT) – mean (stop time)] – 50ms. The average reaction time on go trials (GoRT) was defined as the time between trial onset and pressing the finger from the switch. A GoRT of 800ms reflects a response on the target. By using a participant-specific stop time, the degree of stopping difficulty is comparable across participants. By subtracting 50ms, we ensured >50% successful stop trials and sufficient trials for TEP averaging. To keep the participant alert, a small number of stop trials were catch trials (10 trials that were very easy to inhibit, i.e. extra 100ms; 10 trials that were very hard to inhibit, i.e. less 100ms).

The majority of trials (i.e 70%; 560 out of 800 trials) were stimulation trials (either active or sham TMS). There were 70 TMS pulses for each stimulation condition (active or sham), trial type (certain go, uncertain go, stop trial), and pulse timing (early, late). The trial duration was 3.5, 4 or 4.5s depending on the time point of stimulation in the previous and current trial, such that there was at least 3.5s between two consecutive TMS pulses. Non-stimulated trials comprised 20 certain go, 200 uncertain go and 20 stop trials. Sufficient breaks were provided to participants based on their individual pace, and it took about 1h to complete all four task blocks.

Data analysis

Task data processing

Behavioral analysis was performed on the baseline task session without TMS. GoRTs shorter than 400ms (i.e., early responses) or longer than 1000ms (i.e., no response) were considered errors and removed from the analyses [42-44]. Proactive inhibition was calculated as the amount of response slowing (goRT) in uncertain go compared to certain go trials. Reactive inhibition was calculated as the stop-signal reaction time (SSRT) via the integration method (and go omissions were replaced with the maximum RT of 1000ms) [2].

TMS-EEG data processing

Data preprocessing

All data processing was performed in EEGLAB (v2021.1), using the TMS-EEG signal analyzer toolbox (TESA 1.1.1) [45] on the MATLAB 2021b platform (MathWorks®, Inc., Massachusetts, USA). We followed a processing pipeline based on recommendations from Bertazzoli et al. [46] and Rogasch et al. [47]. Before commencing the data processing, we merged the active and sham TMS blocks for the same target into a single datafile. Bad channels (saturated or noisy) were removed. TMS-EEG data was then epoched around each TMS pulse (-1000 to 1000ms) and baseline-corrected to the pre-TMS pulses period (-200 to -10ms). To remove the large initial artifact of the TMS pulse, we discarded the data 4 to 10ms before and after the TMS pulse, followed by cubic interpolation over a 20ms window.

The data was subsequently downsampled from 5000 to 1000Hz. We then visually inspected and removed bad trials. An initial independent component analysis (FastICA) [48] was applied to remove TMS-related artifacts (muscle, eye blink, decay and recharging artifacts [45]). After performing bandpass filter from 1 to 100Hz and bandstop filter from 48 to 52Hz (remove non-neural data and line noise), we applied a second round of fastICA to eliminate remaining artifacts, such as eye movements and blinks, muscle and electrode artifacts (Rogasch et al., 2017). Bad channels were then interpolated using spherical interpolation. Lastly, the data was re-referenced using the average of all channels. The non-stimulated trials followed the same preprocessing steps with epoching about virtual TMS event markers (omitting steps related to the TMS artifact and the first ICA).

TEP peak analysis

TEPs were calculated by averaging across trials for each condition. We defined the channel closest to the target site as region of interest to extract the TEP waveform, which was C3 for M1 and FC2 for preSMA. The TEP peak amplitude in a prespecified window (N15 (10-20ms), P30 (20-40ms), N45 (30-60ms), P60 (40-80ms), N100 (80-140ms) and P180 (160-240ms) were then extracted. If no peak was found within the window, the amplitude at the center timepoint was defined as the amplitude for that peak (e.g., the TEP amplitude at 45ms would be defined as N45 if there was no exact N45).

ERP analysis

Stimulus-locked event-related potentials (ERPs) were created for go trials (time-locked to the average SSD) and stop trials (time-locked to the SSD). We identified the peak of the P2, N2 and P3 by identifying the maximum trough or peak within the window of interest (180-400ms following the stop-signal).

Statistical analysis

Differences in baseline task performance between active and sham TMS conditions were examined using paired-T test. Statistical analysis for TEP peaks was performed in MATLAB 2021b platform (MathWorks®, Inc., Massachusetts, USA) and R (v4.3.3). Repeated measures analysis of variance (rANOVA) was applied to investigate the main effects (TMS type (active and sham) and Trial type (successful stops and uncertain goes for late TMS, and uncertain and certain go trials for early TMS)) and their interaction for early and late TMS, respectively. Post hoc multiple comparisons were conducted by using paired t-tests with Bonferroni correction. Pearson correlations were performed to test for a relationship between TEP peak amplitude and the baseline task performance. The Scheirer-Ray-Hare test (non-parametric rANOVA) was applied to compare the VAS rank values. The level of significance used for all the tests was $p < 0.05$.

Results

Task performance

All participants tolerated the stimulation well as indicated by the low VAS scores with respect to pain (on average 2.15 for M1 and 1.45 for preSMA, Table S1). One participant was excluded from further analyses due to a low successful stop rate in the baseline task (< 30%) resulting in a final sample of 24 participants. The overview of task performance is presented in Table 2. Omissions and errors for go trials were infrequent (typically below 2%) and did not show main effects of target site (M1 or preSMA) or TMS type (active or sham). Nevertheless, omission rates on uncertain go trials were significantly higher during active TMS in M1 than preSMA. The stop success rate was significantly lower during active than sham TMS and especially low for active M1 stimulation, possibly due to an involuntary finger movement induced by the TMS pulse.

Table 2. Task performance for different conditions

Conditions	Baseline task	M1		preSMA		Effect		
		Active TMS	Sham TMS	Active TMS	Sham TMS	target	TMS type	target * TMS type
Successful stop rate (%)	50.92 ± 1.67	67.86 ± 11.71	79.64 ± 10.32	81.25 ± 8.38	80.94 ± 7.43	**F = 30.974, p < 0.001**[#]	**F = 33.099, p < 0.001**[#]	**F = 31.161, p < 0.001**[#]
SSD (ms)*	604.58 ± 16.26	561.33 ± 16.26	561.33 ± 16.26	561.33 ± 16.26	561.33 ± 16.26			
Failed stop RT (ms)	802.47 ± 12.27							
SSRT (ms)	215.83 ± 11.99							
Mean certainGO RT (ms)	811.48 ± 7.90							
certainGO omission (%)	0.1 ± 0.50	0.68 ± 0.97	0.31 ± 0.55	0.73 ± 1.47	0.47 ± 0.89	F = 0.695, p = 0.695	F = 0.062, p = 0.062	F = 0.753, p = 0.753
certainGO errors (%)	0	0.16 ± 0.56	0	0	0.10 ± 0.35	F = 0.138, p = 0.714	F = 0.138, p = 0.714	F = 4.021, p = 0.057
Mean uncertainGO RT (ms)	822.96 ± 9.99							
uncertainGO omission (%)	0.39 ± 0.68	2.22 ± 2.78	1.41 ± 1.48	1.48 ± 1.72	1.89 ± 2.03	F = 0.29, p = 0.595	F = 0.619, p = 0.439	**F = 4.779, p = 0.039**[#]
uncertainGO errors (%)	0	0.09 ± 0.21	0.05 ± 0.19	0.02 ± 0.09	0.02 ± 0.09	F = 3.286, p = 0.083	F = 0.324, p = 0.575	F = 0.324, p = 0.575
Proactive slowing (ms)	11.48 ± 10.29							

* During the baseline task SSD was adapted on a trial-by-trial basis (±25ms) to reach a 50% success level on stop trials. During TMS the SSD was fixed to the average SSD of the baseline task – 50ms. [#] **Bold text** indicates statistically significant results ($p < 0.05$).

TEP at rest

Active TMS on M1 increased N15, P30 and P60 amplitude at rest. Active TMS on preSMA amplified N45 and N100 amplitude, in comparison to sham stimulation (Figure 2A, Table S2).

Across participants, baseline SSRTs were associated with the difference in TEP amplitude between active and sham M1 stimulation. A larger P30 difference was associated with slower SSRTs ($r = 0.546$, $p = 0.016$) whereas a larger N45 difference was related to faster SSRTs ($r = 0.498$, $p = 0.026$). These relationships were mostly localized to the stimulation site (Figure 2B).

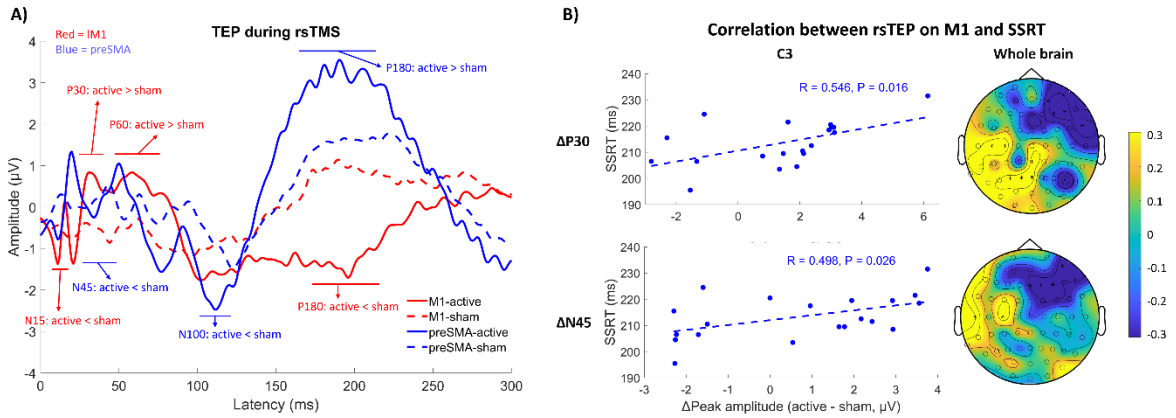

Figure 2. TEP during rsTMS (N = 22). **(A)** TEP time course and the peak amplitude comparison between active (solid line) and sham (dashed line) stimulation on M1 (red) and preSMA (blue) in rest ($p < 0.05$). **(B)** Correlation between ΔP30 and ΔN45 amplitude (active - sham) and baseline SSRT on M1 (C3) and for the whole brain. Positive correlations between ΔP30, ΔN45 and SSRT showed the mostly highest correlation through the whole brain on C3. The yellow and blue represent positive and negative correlations in the topologic plots.

TEP during task performance

Early time point

Early M1 stimulation (i.e. 300ms after trial onset) resulted in higher N15, P60, and N100 amplitudes compared to sham stimulation (Figure 3A, Table 3). Similarly, early TMS on preSMA led to greater N15, N100 and P180 amplitudes under active stimulation compared to sham (Figure 3B). For early preSMA stimulation, the N15 amplitude also demonstrated a main effect of Trial type, with higher amplitudes observed in uncertain go trials compared to certain go trials. A similar pattern was visible for N45 and N100 albeit not significant ($p = 0.06$).

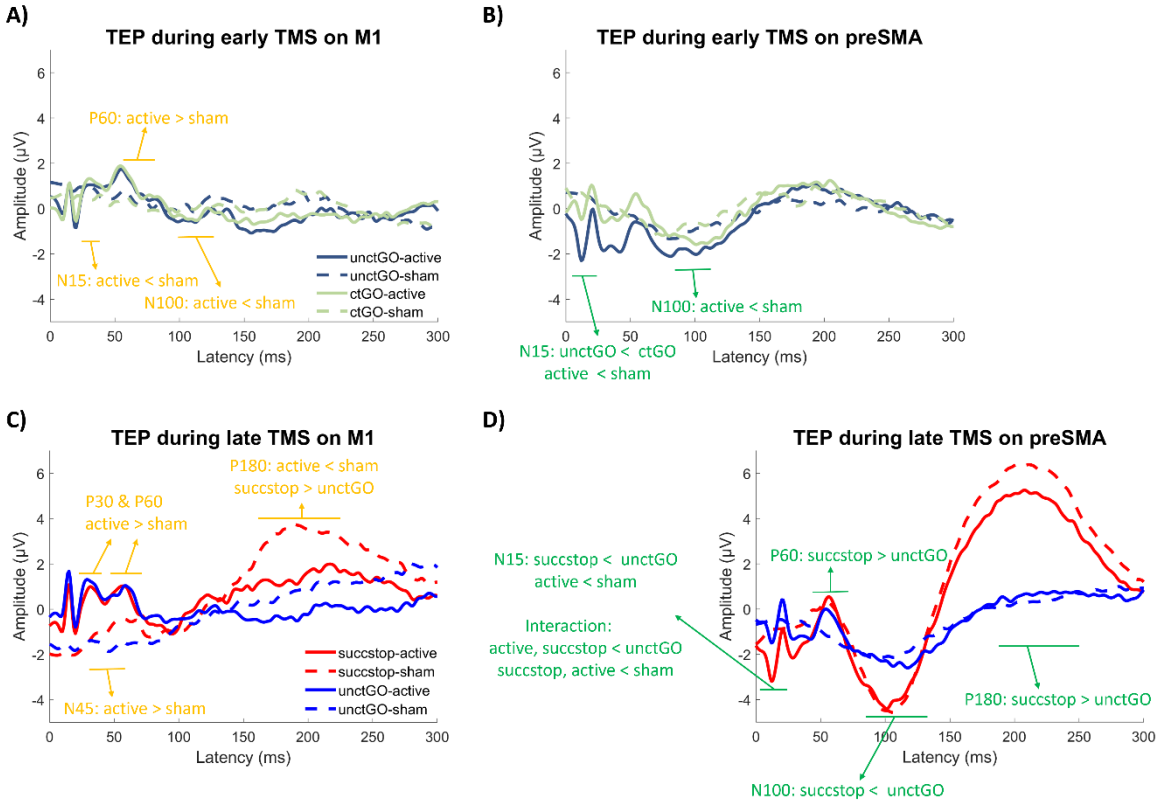

Figure 3. TEP during task performance (N = 24). The time course for early TMS on **(A)** M1 and **(B)** preSMA was plotted separately. Significant effects for rANOVA were highlighted in yellow for M1 and in green text for preSMA, consistent across all panels. The displays of the time course on **(C)** M1 and **(D)** preSMA under late TMS were shown in the lower panels.

Table 3. TEP peak amplitude for early TMS during task performance

Target	TEP peak	Uncertain go trials		Certain go trials		Effect		
		Active TMS	**Sham TMS**	**Active TMS**	**Sham TMS**	**Trial type**	**TMS type**	**Trial type * TMS type**
M1	N15	-2.40 ± 4.50	0.64 ± 1.43	-2.82 ± 6.36	0.27 ± 1.76	F = 0.534, p = 0.472	**F = 11.428, p = 0.003**[#]	F = 0.02, p = 0.965
	P30	2.10 ± 2.83	1.44 ± 1.83	2.21 ± 3.63	1.15 ± 1.97	F = 0.660, p = 0.800	F =1.903, p = 0.181	F = 0.376, p = 0.546
	N45	-0.10 ± 2.73	-0.14 ± 1.77	0.34 ± 3.33	-0.35 ± 1.45	F = 0.193, p = 0.665	F = 0.442, p = 0.513	F = 1.343, p = 0.258
	P60	2.87 ± 3.21	1.30 ± 2.35	3.20 ± 2.74	1.18 ± 1.71	F = 0.104, p = 0.750	**F = 7.191, p = 0.013**[#]	F = 0.505, p = 0.485
	N100	-2.07 ± 2.74	-0.95 ± 1.16	-1.83 ± 2.11	-0.98 ± 0.84	F = 0.171, p = 0.683	**F = 4.467, p = 0.046**[#]	F = 0.401, p = 0.533
	P180	1.08 ± 1.80	1.35 ± 1.46	1.14 ± 1.71	1.44 ± 1.29	F = 0.313, p = 0.282	F = 0.567, p = 0.459	F = 0.004, p = 0.948
preSMA	N15	-2.63 ± 4.40	0.30 ± 1.50	-0.86 ± 2.52	0.48 ± 2.27	**F = 4.264, p = 0.05**[#]	**F = 14.213, p = 0.001**[#]	F = 2.472, p = 0.130
	P30	-0.03 ± 2.91	0.50 ± 1.40	0.89 ± 2.52	0.49 ± 1.53	F = 1.038, p = 0.319	F = 0.024, p = 0.878	F = 1.187, p = 0.287
	N45	-2.52 ± 3.42	-0.79 ± 1.64	-1.15 ± 2.60	-0.73 ± 1.52	F = 3.943, p = 0.059	F = 3.352, p = 0.080	F = 3.925, p = 0.060
	P60	0.44 ± 2.82	0.26 ± 1.48	1.59 ± 1.86	0.33 ± 1.45	F = 3.418, p = 0.077	F = 2.402, p = 0.135	F = 2.624, p = 0.119
	N100	-2.97 ± 2.15	-1.93 ± 1.39	-2.66 ± 1.68	-1.61 ± 1.87	F = 3.928, p = 0.060	**F = 5.277, p = < 0.001**[#]	F = 0.002, p = 0.968
	P180	2.08 ± 1.67	1.15 ± 0.96	2.36 ± 1.63	1.77 ± 1.34	**F = 6.100, p = 0.021**[#]	**F = 6.085, p = 0.022**[#]	F = 1.274, p = 0.271

Mean ± SD was reported for TEP peak amplitude. [#] **Bold text** indicates statistically significant results ($p < 0.05$).

Late time point

TMS targeting M1 showed a main effect of TMS type. Specifically, active late TMS on M1 increased P30, N45, P60 and P180 amplitude compared to sham (Figure 3C, Table 4). In addition, P180 amplitude was significantly higher in successful stop trials compared to go trials. However, no interaction between Trial type and TMS type was found.

In contrast, late TMS on preSMA primarily elicited the main effect of Trial type, with increased N15, P60, N100 and P180 amplitudes observed in successful stop trials than uncertain go trials (Figure 3D). The N15 amplitude also exhibited a main effect of TMS type, with greater amplitude during active stimulation. Notably, an interaction between Trial type and TMS type was observed for N15. Post hoc analysis indicated a Trial type difference solely under active stimulation, with greater N15 amplitude in successful stop than uncertain go trials ($p = 0.05$). Moreover, within successful stop trials, the N15 amplitude was significantly higher under active TMS compared to sham stimulation ($p = 0.001$).

Table 4. TEP peak amplitude for late TMS during task performance.

Target	TEP peak	Successful stop trials		Uncertain go trials		Effect		
		Active TMS	**Sham TMS**	**Active TMS**	**Sham TMS**	**Trial type**	**TMS type**	**Trial type * TMS type**
M1	N15	-2.58 ± 3.40	-2.28 ± 1.46	-1.91 ± 4.33	-1.95 ± 2.21	F = 2.184, p = 0.153	F = 0.042, p = 0.839	F = 0.184, p = 0.672
	P30	1.45 ± 2.98	-0.78 ± 1.87	1.98 ± 3.54	-0.95 ± 1.81	F =0.295, p = 0.592	**F = 15.126, p = 0.001**[#]	F = 1.643, p = 0.213
	N45	-0.23 ± 3.80	-1.80 ± 1.46	-0.36 ± 3.79	-2.32 ± 1.70	F = 0.839, p = 0.369	**F = 6.332, p = 0.019**[#]	F = 0.431, p = 0.518
	P60	2.25 ± 3.08	0.18 ± 1.42	2.16 ± 4.04	-0.56 ± 1.63	F = 1.326, p = 0.261	**F = 11.026, p = 0.003**[#]	F = 0.622, p = 0.438
	N100	-1.84 ± 3.75	-1.86 ± 2.44	-2.01 ± 2.25	-1.75 ± 2.32	F = 0.005, p = 0.944	F =0.034, p = 0.856	F = 0.118, p = .0734
	P180	3.26 ± 3.05	4.78 ± 1.88	1.26 ± 2.69	2.17 ± 2.61	**F = 17.531, p < 0.001**[#]	**F = 16.360, p = 0.001**[#]	F =0.257, p = 0.617
preSMA	N15	-3.46 ± 4.00	-1.07 ± 1.85	-1.82 ± 3.57	-0.65 ± 1.51	**F = 9.208, p = 0.006**[#]	**F = 6.093, p = 0.021**[#]	**F = 4.638, p = 0.042**[#]
	P30	-0.57 ± 2.65	-0.41 ± 1.58	0.08 ± 2.98	-0.18 ± 1.52	F = 2.210, p = 0.151	F = 0.009, p = 0.926	F = 0.861, p = 0.363
	N45	-1.81 ± 3.38	-0.72 ± 2.43	-2.06 ± 2.68	-1.33 ± 1.10	F = 1.323, p = 0.262	F = 1.926, p = 0.178	F = 0.539, p = 0.470
	P60	1.05 ± 1.89	0.91 ± 2.05	0.55 ± 2.15	-0.59 ± 1.33	**F = 7.17, p = 0.013**[#]	F = 3.416, p = 0.077	F = 3.031, p = 0.095
	N100	-5.49 ± 3.68	-5.60 ± 4.08	-3.43 ± 2.56	-2.57 ± 1.83	**F = 40.75, p < 0.001**[#]	F = 0.264, p = 0.612	F = 2.582, p = 0.122
	P180	6.59 ± 4.37	7.58 ± 4.99	1.60 ± 1.52	1.27 ± 1.80	**F = 42.895, p = 0.000**[#]	F = 0.430, p = 0.519	F = 1.602, p = 0.218

Mean ± SD was reported for TEP peak amplitude. [#] **Bold text** indicates statistically significant results ($p < 0.05$).

ERP for no-stimulation trials during task

Prominent P2, N2 and P3 peaks were observed following the stop-signal for both M1 and preSMA (Figure 4, Table S3). Notably, there is a high degree of temporal overlap between the stop-signal related P2 and TEP P60, between the N2 and TEP N100, and between the P3 and the TEP P180 (Figure 4). Despite this overlap, no significant correlation was found between the corresponding TEP and ERP amplitudes (Table S3). The rsTEP showed an intriguingly similar pattern to the taskTEP and ERP on preSMA. This suggested that the preSMA may have a stable baseline excitability or network state that does not dramatically change regardless of the task state.

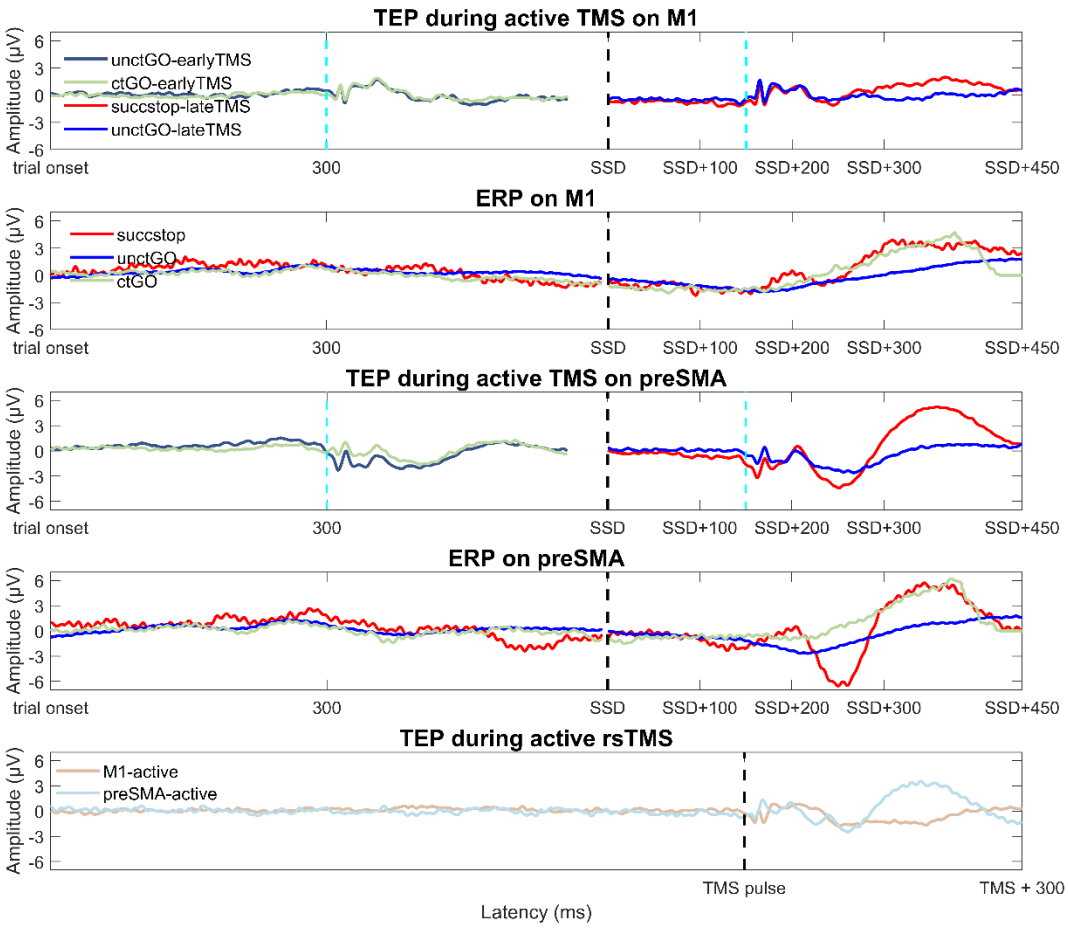

Figure 4. ERP and TEP time course in the time domain. The time courses for TEP and ERP under different conditions were aligned to start at the trial onset. During task performance, early TMS was applied 300ms after trial onset, while late TMS was delivered 150ms after individual SSD. The TMS pulse was indicated by cyan dotted lines, and the group average SSD for stop trials was represented by black dotted lines. The TEP components P60, N100, and P180 corresponded to ERP components P2, N2, and P3, respectively. In terms of the TEP at rest, the TMS pulse was aligned with late TMS. The rsTEP in preSMA mirrored the pattern observed during task performance.

Discussion

This study combined TMS-EEG to probe GABA- and glutamatergic signaling during reactive and proactive motor inhibition. Importantly, compared to ppTMS, spTMS does not require a substantial delay between pulses (e.g. LICI), making it possible to study both GABAa and GABAb involvement as the reactive inhibition process unfolds. In addition, TMS-EEG allows to investigate receptor activity across the cortex, not being restricted to M1. Here we also targeted preSMA, providing a more complete understanding of GABAergic and glutamatergic signaling in the wider motor inhibition network during reactive and proactive inhibition.

GABAa levels in rest predict reactive inhibition performance

The relationship between M1 N45 peak amplitude at rest and SSRT suggests that GABAa supports reactive inhibition. This finding is in line with previous studies demonstrating that individuals with higher rest SICI are more efficient at inhibiting prepotent actions [16, 49-51]. Opposed to TMS-EMG, it is possible to look beyond M1 with TMS-EEG. The whole brain correlation plot revealed that the relation between N45 and SSRT was confined to the sensory-motor areas. Additionally, higher excitatory P30 amplitudes at M1 during rest were associated with slower SSRTs. P30 is thought to represent a local excitatory response [20, 52, 53] and is reduced after paired pulse TMS with and ISI of 3ms (SICI protocol) compared to spTMS [54, 55]. This highlights that the TEP peaks are likely not dominated by a single neurotransmitter, reflecting independent mechanism, but rather depending on the ratio of GABA to glutamate [56, 57].

Early TEP peak N15 is larger during successful stopping

To assess changes in TEP amplitude during successful reactive inhibition TMS was applied 150ms after the stop-signal. During this time window, inhibition is implemented and starts to become evident as reduced MEP amplitude in the effector agonist muscle [7, 9, 58]. N15 peak amplitude was significantly larger during successful stopping when active TMS was applied over preSMA. This early TEP component is typically localized over and near the target site [22, 24, 25, 39, 59, 60] and is believed to reflect excitation [24, 39]. The preSMA plays a crucial role in reactive stopping by rapidly sending excitatory signals to the STN via the hyperdirect pathway, ultimately, leading to the suppression of motor output [4, 61]. We hypothesize that stronger early excitation in the preSMA enhances the initiation of inhibitory processes mediated by cortico-subcortical interaction.

No interaction was found for N45 or N100 peak amplitude in preSMA or M1, suggesting that neither GABAa nor GABAb signaling increased during reactive inhibition. Especially for N45 the

absence of an effect is surprising. M1 N45 amplitude at rest correlated with SSRT, and SICI assessed at the same timepoint increases during successful stopping [7, 62]. One possible explanation is that task-TMS interactions at these later timepoints are obscured by temporal overlap in the TEP and event-related potentials generated in response to the stop-signal.

Disentangling TMS evoked potentials from ERP

Despite the limited amount of trials without TMS stimulation (20 stop trials and 100 go trials), we were able to identify clear P2, N2 and P3 ERP components as typically observed in stop compared to go trials [63, 64]. Comparing the ERP with the TEP in the preSMA, and to a lesser extent also on M1, reveals a clear overlap in peak timings from approximately 50ms after the TMS pulse, i.e., 200ms after the stop signal was presented (Figure 4). There also seem to be only task induced effect in the TEP (stop>go) from this moment onwards (~50ms after the TMS pulse) and no differences between sham and active TMS (Figure 3C+D). This suggests that the evoked response to the stop-signal was so strong that any small TMS effect became unobservable. It also raises the question whether the TEP during successful stopping and the ERP might share generating mechanisms, such as thalamocortical dynamics [65], making it difficult to fully disentangle TMS evoked potentials from ongoing event-related responses during a task.

PreSMA supports proactive inhibition

When there is a possible need for motor inhibition, participants tend to slow down in order to increase the likelihood of being able to inhibit their movement. In the present study, the response times of go trials in which a stop-signal could appear compared to certain go trials showed the expected proactive slowing [66]. Previous TMS studies utilizing a paired-pulse paradigm over M1 found higher LICI in go trials where stopping might be required [62]. Here, we observed significant differences in peak amplitude between active and sham TMS on M1, but there was no difference between certain and uncertain go trials or an interaction. In rest LICI relates to the slope of the N100 [20, 67], therefore one would expect higher N100 amplitudes during uncertain versus certain go trials. This null result cannot be explained by event-related potential clouding the TEP (Figure 4). Therefore, it raises the question whether LICI and N100 reflect the same inhibitory activity in this task context.

In contrast, preSMA N15 amplitudes displayed a main effect of TMS type and Trial type, with higher amplitudes for active TMS and uncertain go trials. This suggests that similarly to reactive inhibition, preSMA recruits the motor inhibition network for proactive inhibition with an early excitatory signal. N45 and N100 showed a similar picture, although the Trial type effect was not significant ($p = 0.06$), implying that both GABAa and GABAb signaling might play a role in proactive

inhibition and are not exclusive to the motor cortex. Possibly the increase in GABAergic signaling in preSMA during motor inhibition is related to an increase in beta oscillatory activity. Beta activity is believed to arise from spiking interactions between pyramidal cells and GABAergic interneurons [68-72], as the administration of GABAergic receptor agonists has been shown to increase beta power in the brain [68, 73-75]. Increased beta activity is observed throughout the entire motor inhibition network during successful reactive inhibition [43, 76-78] and proactive inhibition [79, 80] and is believed to facilitate inter-regional communication [81, 82].

Limitations

This study has few methodological limitations. First, administering TMS pulses 150ms after the stop-signal on both M1 and preSMA might have been too late for preSMA, based on recent insights that stop command from preSMA might be transferred to motor cortex ~120ms after stop signal [58]. Second, the stimulation intensity for preSMA might have been insufficient due to its deeper cortical position. While preSMA stimulation elicited smaller amplitude changes in early TEP components at rest compared to M1 stimulation, the intensity may have been adequate during task performance when the area was actively engaged. Finally, the stop signals on TMS trials were presented 50ms earlier than individual stop signal delays during baseline task performance. This ensured more successful stop trials for TEP analysis and avoided stimulating after movement onset on go trials. However, by making the task easier, participants might engage in less reactive stop process than they would with stop signal delays matching their SSRT.

Conclusion

The present study provides novel insights into the neural mechanisms of motor inhibition by combining TMS with EEG. Unlike conventional TMS-EMG measures that solely focus on M1, TMS-EEG enables investigation of GABA- and glutamatergic receptor involvement across the cortex. By stimulating preSMA, a key node within the motor inhibition network, we observed increased N15 amplitudes during both reactive and proactive inhibition. This likely reflects fast excitatory signals from preSMA towards the basal ganglia to initiate or implement motor inhibition. Additionally, GABAa and GABAb receptor activation increased in preSMA during proactive inhibition, demonstrating that GABAergic signaling is not exclusive to the motor cortex during inhibition.

Reference

[1] Duque J, Greenhouse I, Labruna L, Ivry RB. Physiological Markers of Motor Inhibition during Human Behavior. Trends Neurosci. 2017;40(4):219-36. https://doi.org/10.1016/j.tins.2017.02.006.

[2] Verbruggen F, Aron AR, Band GP, Beste C, Bissett PG, Brockett AT, et al. A consensus guide to capturing the ability to inhibit actions and impulsive behaviors in the stop-signal task. Elife. 2019;8:e46323. https://doi.org/10.7554/eLife.46323.

[3] Aron AR. From reactive to proactive and selective control: developing a richer model for stopping inappropriate responses. Biol Psychiatry. 2011;69(12):e55-68. https://doi.org/10.1016/j.biopsych.2010.07.024.

[4] Jahanshahi M, Obeso I, Rothwell JC, Obeso JA. A fronto-striato-subthalamic-pallidal network for goal-directed and habitual inhibition. Nat Rev Neurosci. 2015;16(12):719-32. https://doi.org/10.1038/nrn4038.

[5] Stinear CM, Coxon JP, Byblow WD. Primary motor cortex and movement prevention: where Stop meets Go. Neurosci Biobehav Rev. 2009;33(5):662-73. https://doi.org/10.1016/j.neubiorev.2008.08.013.

[6] Badry R, Mima T, Aso T, Nakatsuka M, Abe M, Fathi D, et al. Suppression of human cortico-motoneuronal excitability during the Stop-signal task. Clin Neurophysiol. 2009;120(9):1717-23. https://doi.org/10.1016/j.clinph.2009.06.027.

[7] Coxon JP, Stinear CM, Byblow WD. Intracortical inhibition during volitional inhibition of prepared action. J Neurophysiol. 2006;95(6):3371-83. https://doi.org/10.1152/jn.01334.2005.

[8] van den Wildenberg WP, Burle B, Vidal F, van der Molen MW, Ridderinkhof KR, Hasbroucq T. Mechanisms and dynamics of cortical motor inhibition in the stop-signal paradigm: a TMS study. J Cogn Neurosci. 2010;22(2):225-39. https://doi.org/10.1162/jocn.2009.21248.

[9] MacDonald HJ, Coxon JP, Stinear CM, Byblow WD. The fall and rise of corticomotor excitability with cancellation and reinitiation of prepared action. J Neurophysiol. 2014;112(11):2707-17. https://doi.org/10.1152/jn.00366.2014.

[10] Hermans L, Leunissen I, Pauwels L, Cuypers K, Peeters R, Puts NAJ, et al. Brain GABA Levels Are Associated with Inhibitory Control Deficits in Older Adults. J Neurosci. 2018;38(36):7844-51. https://doi.org/10.1523/JNEUROSCI.0760-18.2018.

[11] Chowdhury NS, Livesey EJ, Harris JA. Stop Signal Task Training Strengthens GABA-mediated Neurotransmission within the Primary Motor Cortex. J Cogn Neurosci. 2020;32(10):1984-2000. https://doi.org/10.1162/jocn_a_01597.

[12] Terunuma M. Diversity of structure and function of GABA(B) receptors: a complexity of GABA(B)-mediated signaling. Proc Jpn Acad Ser B Phys Biol Sci. 2018;94(10):390-411. https://doi.org/10.2183/pjab.94.026.

[13] Cowie MJ, MacDonald HJ, Cirillo J, Byblow WD. Proactive modulation of long-interval intracortical inhibition during response inhibition. J Neurophysiol. 2016;116(2):859-67. https://doi.org/10.1152/jn.00144.2016.

[14] Paci M, Di Cosmo G, Perrucci MG, Ferri F, Costantini M. Cortical silent period reflects individual differences in action stopping performance. Sci Rep. 2021;11(1):15158. https://doi.org/10.1038/s41598-021-94494-w.

[15] He Q, Geissler CF, Ferrante M, Hartwigsen G, Friehs MA. Effects of transcranial magnetic stimulation on reactive response inhibition. Neurosci Biobehav Rev. 2024;157:105532. https://doi.org/10.1016/j.neubiorev.2023.105532.

[16] Loomes M, Tran DMD, Chowdhury NS, Birney DP, Harris JA, Livesey EJ. Is cortical inhibition in primary motor cortex related to executive control? Cortex. 2023;160:100-14. https://doi.org/10.1016/j.cortex.2022.12.013.

[17] Chung SW, Rogasch NC, Hoy KE, Fitzgerald PB. Measuring Brain Stimulation Induced Changes in Cortical Properties Using TMS-EEG. Brain Stimul. 2015;8(6):1010-20. https://doi.org/10.1016/j.brs.2015.07.029.

[18] Tremblay S, Rogasch NC, Premoli I, Blumberger DM, Casarotto S, Chen R, et al. Clinical utility and prospective of TMS-EEG. Clin Neurophysiol. 2019;130(5):802-44. https://doi.org/10.1016/j.clinph.2019.01.001.

[19] Gordon PC, Song YF, Jovellar DB, Rostami M, Belardinelli P, Ziemann U. Untangling TMS-EEG responses caused by TMS versus sensory input using optimized sham control and GABAergic challenge. J Physiol. 2023;601(10):1981-98. https://doi.org/10.1113/JP283986.

[20] Rogasch NC, Daskalakis ZJ, Fitzgerald PB. Mechanisms underlying long-interval cortical inhibition in the human motor cortex: a TMS-EEG study. J Neurophysiol. 2013;109(1):89-98. https://doi.org/10.1152/jn.00762.2012.

[21] Rogasch NC, Fitzgerald PB. Assessing cortical network properties using TMS-EEG. Hum Brain Mapp. 2013;34(7):1652-69. https://doi.org/10.1002/hbm.22016.

[22] Darmani G, Ziemann U. Pharmacophysiology of TMS-evoked EEG potentials: A mini-review. Brain Stimul. 2019;12(3):829-31. https://doi.org/10.1016/j.brs.2019.02.021.

[23] Farzan F. Transcranial Magnetic Stimulation-Electroencephalography for Biomarker Discovery in Psychiatry. Biol Psychiatry. 2024;95(6):564-80. https://doi.org/10.1016/j.biopsych.2023.12.018.

[24] Maki H, Ilmoniemi RJ. The relationship between peripheral and early cortical activation induced by transcranial magnetic stimulation. Neurosci Lett. 2010;478(1):24-8. https://doi.org/10.1016/j.neulet.2010.04.059.

[25] Esser SK, Huber R, Massimini M, Peterson MJ, Ferrarelli F, Tononi G. A direct demonstration of cortical LTP in humans: a combined TMS/EEG study. Brain Res Bull. 2006;69(1):86-94. https://doi.org/10.1016/j.brainresbull.2005.11.003.

[26] Premoli I, Castellanos N, Rivolta D, Belardinelli P, Bajo R, Zipser C, et al. TMS-EEG signatures of GABAergic neurotransmission in the human cortex. J Neurosci. 2014;34(16):5603-12. https://doi.org/10.1523/JNEUROSCI.5089-13.2014.

[27] Darmani G, Zipser CM, Bohmer GM, Deschet K, Muller-Dahlhaus F, Belardinelli P, et al. Effects of the Selective alpha5-GABAAR Antagonist S44819 on Excitability in the Human Brain: A TMS-EMG and TMS-EEG Phase I Study. J Neurosci. 2016;36(49):12312-20. https://doi.org/10.1523/JNEUROSCI.1689-16.2016.

[28] Yamanaka K, Kadota H, Nozaki D. Long-latency TMS-evoked potentials during motor execution and inhibition. Front Hum Neurosci. 2013;7:751. https://doi.org/10.3389/fnhum.2013.00751.

[29] Oldfield RC. The assessment and analysis of handedness: The Edinburgh inventory. Neuropsychologia. 1971;9(1):97-113.

[30] Rossi S, Hallett M, Rossini PM, Pascual-Leone A, Safety of TMSCG. Safety, ethical considerations, and application guidelines for the use of transcranial magnetic stimulation in clinical practice and research. Clin Neurophysiol. 2009;120(12):2008-39. https://doi.org/10.1016/j.clinph.2009.08.016.

[31] Rydalch G, Bell HB, Ruddy KL, Bolton DAE. Stop-signal reaction time correlates with a compensatory balance response. Gait Posture. 2019;71:273-8. https://doi.org/10.1016/j.gaitpost.2019.05.015.

[32] Rossini PM, Barker AT, Berardelli A, Caramia MD, Caruso G, Cracco RQ, et al. Non-invasive electrical and magnetic stimulation of the brain, spinal cord and roots: basic principles and procedures for routine clinical application. Report of an IFCN committee. Electroencephalogr Clin Neurophysiol. 1994;91(2):79-92. https://doi.org/10.1016/0013-4694(94)90029-9.

[33] Wang L, Yu C, Chen H, Qin W, He Y, Fan F, et al. Dynamic functional reorganization of the motor execution network after stroke. Brain. 2010;133(Pt 4):1224-38. https://doi.org/10.1093/brain/awq043.

[34] Power JD, Cohen AL, Nelson SM, Wig GS, Barnes KA, Church JA, et al. Functional network organization of the human brain. Neuron. 2011;72(4):665-78. https://doi.org/10.1016/j.neuron.2011.09.006.

[35] Casula EP, Pellicciari MC, Bonni S, Borghi I, Maiella M, Assogna M, et al. Decreased Frontal Gamma Activity in Alzheimer Disease Patients. Ann Neurol. 2022;92(3):464-75. https://doi.org/10.1002/ana.26444.

[36] Conde V, Tomasevic L, Akopian I, Stanek K, Saturnino GB, Thielscher A, et al. The non-transcranial TMS-evoked potential is an inherent source of ambiguity in TMS-EEG studies. NeuroImage. 2019;185:300-12. https://doi.org/10.1016/j.neuroimage.2018.10.052.

[37] Massimini M, Ferrarelli F, Huber R, Esser SK, Singh H, Tononi G. Breakdown of cortical effective connectivity during sleep. Sci. 2005;309(5744):2228-32. https://doi.org/10.1126/science.1117256.

[38] Gordon P, Jovellar D, Song Y, Zrenner C, Belardinelli P, Siebner H, et al. Recording brain responses to TMS of primary motor cortex by EEG – utility of an optimized sham procedure. NeuroImage. 2021;245118708. https://doi.org/10.1016/j.neuroimage.2021.118708.

[39] ter Braack EM, de Vos CC, van Putten MJ. Masking the Auditory Evoked Potential in TMS-EEG: A Comparison of Various Methods. Brain Topogr. 2015;28(3):520-8. https://doi.org/10.1007/s10548-013-0312-z.

[40] Lin YY, Shih YH, Chen JT, Hsieh JC, Yeh TC, Liao KK, et al. Differential effects of stimulus intensity on peripheral and neuromagnetic cortical responses to median nerve stimulation. NeuroImage. 2003;20(2):909-17. https://doi.org/10.1016/S1053-8119(03)00387-2.

[41] Torquati K, Pizzella V, Della Penna S, Franciotti R, Babiloni C, Rossini PM, et al. Comparison between SI and SII responses as a function of stimulus intensity. Neuroreport. 2002;13(6):813-9. https://doi.org/10.1097/00001756-200205070-00016.

[42] Leunissen I, Coxon JP, Swinnen SP. A proactive task set influences how response inhibition is implemented in the basal ganglia. Hum Brain Mapp. 2016;37(12):4706-17. https://doi.org/10.1002/hbm.23338.

[43] Leunissen I, Van Steenkiste M, Heise KF, Monteiro TS, Dunovan K, Mantini D, et al. Effects of beta-band and gamma-band rhythmic stimulation on motor inhibition. iScience. 2022;25(5):104338. https://doi.org/10.1016/j.isci.2022.104338.

[44] Leunissen I, Zandbelt BB, Potocanac Z, Swinnen SP, Coxon JP. Reliable estimation of inhibitory efficiency: to anticipate, choose or simply react? Eur J Neurosci. 2017;45(12):1512-23. https://doi.org/10.1111/ejn.13590.

[45] Rogasch NC, Sullivan C, Thomson RH, Rose NS, Bailey NW, Fitzgerald PB, et al. Analysing concurrent transcranial magnetic stimulation and electroencephalographic data: A review and introduction to the open-source TESA software. NeuroImage. 2017;147:934-51. https://doi.org/10.1016/j.neuroimage.2016.10.031.

[46] Bertazzoli G, Esposito R, Mutanen TP, Ferrari C, Ilmoniemi RJ, Miniussi C, et al. The impact of artifact removal approaches on TMS-EEG signal. NeuroImage. 2021;239:118272. https://doi.org/10.1016/j.neuroimage.2021.118272.

[47] Rogasch NC, Biabani M, Mutanen TP. Designing and comparing cleaning pipelines for TMS-EEG data: A theoretical overview and practical example. J Neurosci Methods. 2022;371:109494. https://doi.org/10.1016/j.jneumeth.2022.109494.

[48] Hyvarinen A, Oja E. Independent component analysis: algorithms and applications. Neural Netw. 2000;13(4-5):411-30. https://doi.org/10.1016/s0893-6080(00)00026-5.

[49] Cardellicchio P, Koch G, Fadiga L, D'Ausilio A. Motor overload: GABAergic index of parallel buffer costs. Brain Stimul. 2021;14(5):1106-8. https://doi.org/10.1016/j.brs.2021.07.061.

[50] Tran DMD, Chowdhury NS, McNair NA, Harris JA, Livesey EJ. Linking cortical and behavioural inhibition: Testing the parameter specificity of a transcranial magnetic stimulation protocol. Brain Stimul. 2020;13(5):1381-3. https://doi.org/10.1016/j.brs.2020.07.010.

[51] Chowdhury NS, Livesey EJ, Blaszczynski A, Harris JA. Variations in response control within at-risk gamblers and non-gambling controls explained by GABAergic inhibition in the motor cortex. Cortex. 2018;103:153-63. https://doi.org/10.1016/j.cortex.2018.03.004.

[52] Rogasch NC, Thomson RH, Daskalakis ZJ, Fitzgerald PB. Short-latency artifacts associated with concurrent TMS-EEG. Brain Stimul. 2013;6(6):868-76. https://doi.org/10.1016/j.brs.2013.04.004.

[53] Farzan F, Bortoletto M. Identification and verification of a 'true' TMS evoked potential in TMS-EEG. J Neurosci Methods. 2022;378:109651. https://doi.org/10.1016/j.jneumeth.2022.109651.

[54] Ferreri F, Pasqualetti P, Maatta S, Ponzo D, Ferrarelli F, Tononi G, et al. Human brain connectivity during single and paired pulse transcranial magnetic stimulation. NeuroImage. 2011;54(1):90-102. https://doi.org/10.1016/j.neuroimage.2010.07.056.

[55] Casula EP, Tarantino V, Basso D, Arcara G, Marino G, Toffolo GM, et al. Low-frequency rTMS inhibitory effects in the primary motor cortex: Insights from TMS-evoked potentials. NeuroImage. 2014;98:225-32. https://doi.org/10.1016/j.neuroimage.2014.04.065.

[56] Belardinelli P, Konig F, Liang C, Premoli I, Desideri D, Muller-Dahlhaus F, et al. TMS-EEG signatures of glutamatergic neurotransmission in human cortex. Sci Rep. 2021;11(1):8159. https://doi.org/10.1038/s41598-021-87533-z.

[57] Du X, Rowland LM, Summerfelt A, Wijtenburg A, Chiappelli J, Wisner K, et al. TMS evoked N100 reflects local GABA and glutamate balance. Brain Stimul. 2018;11(5):1071-9. https://doi.org/10.1016/j.brs.2018.05.002.

[58] Jana S, Hannah R, Muralidharan V, Aron AR. Temporal cascade of frontal, motor and muscle processes underlying human action-stopping. Elife. 2020;9:null. https://doi.org/10.7554/eLife.50371.

[59] Bonato C, Miniussi C, Rossini PM. Transcranial magnetic stimulation and cortical evoked potentials: a TMS/EEG co-registration study. Clin Neurophysiol. 2006;117(8):1699-707. https://doi.org/10.1016/j.clinph.2006.05.006.

[60] Komssi S, Kahkonen S, Ilmoniemi RJ. The effect of stimulus intensity on brain responses evoked by transcranial magnetic stimulation. Hum Brain Mapp. 2004;21(3):154-64. https://doi.org/10.1002/hbm.10159.

[61] Wolpe N, Hezemans FH, Rae CL, Zhang J, Rowe JB. The pre-supplementary motor area achieves inhibitory control by modulating response thresholds. Cortex. 2022;152:98-108. https://doi.org/10.1016/j.cortex.2022.03.018.

[62] Hermans L, Maes C, Pauwels L, Cuypers K, Heise KF, Swinnen SP, et al. Age-related alterations in the modulation of intracortical inhibition during stopping of actions. Aging (Albany N Y). 2019;11(2):371-85. https://doi.org/10.18632/aging.101741.

[63] Kok A, Ramautar JR, De Ruiter MB, Band GP, Ridderinkhof KR. ERP components associated with successful and unsuccessful stopping in a stop-signal task. Psychophysiology. 2004;41(1):9-20. https://doi.org/10.1046/j.1469-8986.2003.00127.x.

[64] Huster RJ, Messel MS, Thunberg C, Raud L. The P300 as marker of inhibitory control - Fact or fiction? Cortex. 2020;132:334-48. https://doi.org/10.1016/j.cortex.2020.05.021.

[65] Diesburg DA, Wessel JR, Jones SR. Biophysical modeling of frontocentral ERP generation links circuit-level mechanisms of action-stopping to a behavioral race model. Neuroscience; 2023.

[66] Vink M, Kaldewaij R, Zandbelt BB, Pas P, du Plessis S. The role of stop-signal probability and expectation in proactive inhibition. Eur J Neurosci. 2015;41(8):1086-94. https://doi.org/10.1111/ejn.12879.

[67] Opie GM, Rogasch NC, Goldsworthy MR, Ridding MC, Semmler JG. Investigating TMS–EEG Indices of Long-Interval Intracortical Inhibition at Different Interstimulus Intervals. Brain Stimul. 2017;10(1):65-74 %U https://linkinghub.elsevier.com/retrieve/pii/S1935861X16302078.

[68] Jensen O, Goel P, Kopell N, Pohja M, Hari R, Ermentrout B. On the human sensorimotor-cortex beta rhythm: sources and modeling. Neuroimage. 2005;26(2):347-55. https://doi.org/10.1016/j.neuroimage.2005.02.008.

[69] Kopell N, Whittington MA, Kramer MA. Neuronal assembly dynamics in the beta1 frequency range permits short-term memory. Proc Natl Acad Sci U S A. 2011;108(9):3779-84. https://doi.org/10.1073/pnas.1019676108.

[70] Kramer MA, Roopun AK, Carracedo LM, Traub RD, Whittington MA, Kopell NJ. Rhythm generation through period concatenation in rat somatosensory cortex. PLoS Comput Biol. 2008;4(9):e1000169. https://doi.org/10.1371/journal.pcbi.1000169.

[71] Lee JH, Whittington MA, Kopell NJ. Top-down beta rhythms support selective attention via interlaminar interaction: a model. PLoS Comput Biol. 2013;9(8):e1003164. https://doi.org/10.1371/journal.pcbi.1003164.

[72] Sherman MA, Lee S, Law R, Haegens S, Thorn CA, Hamalainen MS, et al. Neural mechanisms of transient neocortical beta rhythms: Converging evidence from humans, computational modeling, monkeys, and mice. Proc Natl Acad Sci U S A. 2016;113(33):E4885-94. https://doi.org/10.1073/pnas.1604135113.

[73] Hall SD, Stanford IM, Yamawaki N, McAllister CJ, Ronnqvist KC, Woodhall GL, et al. The role of GABAergic modulation in motor function related neuronal network activity. Neuroimage. 2011;56(3):1506-10. https://doi.org/10.1016/j.neuroimage.2011.02.025.

[74] Muthukumaraswamy SD, Myers JF, Wilson SJ, Nutt DJ, Lingford-Hughes A, Singh KD, et al. The effects of elevated endogenous GABA levels on movement-related network oscillations. Neuroimage. 2013;66:36-41. https://doi.org/10.1016/j.neuroimage.2012.10.054.

[75] Premoli I, Rivolta D, Espenhahn S, Castellanos N, Belardinelli P, Ziemann U, et al. Characterization of GABAB-receptor mediated neurotransmission in the human cortex by paired-

pulse TMS–EEG. NeuroImage. 2014;103:152-62. https://doi.org/10.1523/JNEUROSCI.5089-13.2014.

[76] Wessel JR, Waller DA, Greenlee JD. Non-selective inhibition of inappropriate motor-tendencies during response-conflict by a fronto-subthalamic mechanism. eLife. 2019;8:e42959. https://doi.org/10.7554/eLife.42959.

[77] Castiglione A, Wagner J, Anderson M, Aron AR. Preventing a Thought from Coming to Mind Elicits Increased Right Frontal Beta Just as Stopping Action Does. Cereb Cortex. 2019;29(5):2160-72. https://doi.org/10.1093/cercor/bhz017.

[78] Kuhn AA, Trottenberg T, Kivi A, Kupsch A, Schneider GH, Brown P. The relationship between local field potential and neuronal discharge in the subthalamic nucleus of patients with Parkinson's disease. Exp Neurol. 2005;194(1):212-20. https://doi.org/10.1016/j.expneurol.2005.02.010.

[79] Liebrand M, Pein I, Tzvi E, Kramer UM. Temporal Dynamics of Proactive and Reactive Motor Inhibition. Front Hum Neurosci. 2017;11:204. https://doi.org/10.3389/fnhum.2017.00204.

[80] Soh C, Hynd M, Rangel BO, Wessel JR. Adjustments to Proactive Motor Inhibition without Effector-Specific Foreknowledge Are Reflected in a Bilateral Upregulation of Sensorimotor beta-Burst Rates. J Cogn Neurosci. 2021;33(5):784-98. https://doi.org/10.1162/jocn_a_01682.

[81] Fries P. A mechanism for cognitive dynamics: neuronal communication through neuronal coherence. Trends Cogn Sci. 2005;9(10):474-80. https://doi.org/10.1016/j.tics.2005.08.011.

[82] Fang Z, Sack AT, Leunissen I. The phase of tACS-entrained pre-SMA beta oscillations modulates motor inhibition. Neuroimage. 2024;290:120572. https://doi.org/10.1016/j.neuroimage.2024.120572.